J. Fluid Mech. (1972), *vol.* 51, *part* 4, *pp.* 673–685
Printed in Great Britain

Velocity measurements made with a laser dopplermeter on the turbulent pipe flow of a dilute polymer solution

By M. J. RUDD

Cavendish Laboratory, Cambridge†

(Received 17 June 1970 and in revised form 16 April 1971)

This paper presents some new measurements which have been made on a drag-reducing polymer solution in pipe flow. A novel type of laser dopplermeter, which has been developed by the author, is briefly described and the measurements which have been obtained are given. These results and their implications are then discussed in terms of conventional models for turbulent flow in a pipe. These suggest that the polymer has very little effect upon the turbulent core of the flow, but thickens and stabilizes the viscous sublayer. The turbulent intensity inside the sublayer is unchanged but, owing to its thickening, the velocity fluctuations just outside are greater. There is not a general suppression of turbulence within the sublayer although well inside the sublayer the spanwise velocity component is found to be reduced.

1. Introduction

It has been known for some time that solutions of relatively small concentrations (about 10 to 100 parts per million) of certain polymers have a much lower friction in turbulent flow than the basic solvent. Friction reductions as large as 80 % have been observed. The discovery of this phenomenon is generally attributed to Toms (1949) who was working with a solution of polymethylmethacryalate in monochlorobenzene. A comprehensive survey of this subject has been given by Lumley (1969).

The polymers which give rise to this drag reduction have a high molecular weight and give rise to visco-elastic forces in the solution. However, not all large molecular weight polymers give rise to drag reduction. The drag reduction which is produced by the polymers is found only to be induced above a certain critical wall stress and thereafter increases with wall stress until it reaches saturation. The value of the critical wall stress and the amount of drag reduction at saturation are functions of the molecular parameters of the molecules.

Virk, Merrill, Mickley, Smith & Mollo-Christensen (1967) have made velocity measurements on dilute polymer solutions with a hot-wire anemometer. However the visco-elastic forces, induced by the polymer in the solution, can change the heat-transfer properties from the hot wire and hence may affect its reliability. Therefore measurements have now been made with a laser dopplermeter, which

† Present address: Department of Aeronautics, New York University, University Heights, The Bronx, New York 10453.

is not affected by the fluid. Further, the dopplermeter has a resolution of 10 micrometres and is able to make measurements down to about 50 micrometres from the wall, which is much closer than a hot wire can be used. Accordingly, the region very close to the wall, where the drag reduction is most likely to be caused, can be studied in some detail.

2. The laser dopplermeter

The laser dopplermeter is an instrument which measures the velocity of an object or fluid by means of the Doppler shift of laser light. Much has been published on these instruments (Foreman *et al.* 1966; Goldstein & Krein 1967). The light is scattered from small particles in the fluid and its frequency is changed by the well-known Doppler effect. The frequency shift is very small, typically 1 part in 10^{10}, and cannot be measured spectroscopically. It is measured by

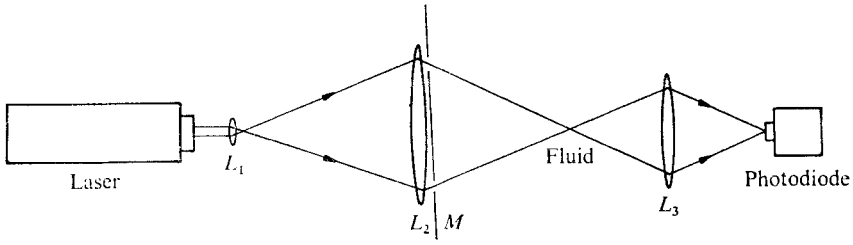

FIGURE 1. Author's optical system: L_1 and L_2, transmitting lenses; M, mask; L_3, receiving lens.

mixing the scattered and original light together and letting them beat at their difference frequency. This is referred to as 'heterodyning'. This beat frequency, around 50 kHz, can then be analysed electronically. The theory is dealt with in the references given above and the Doppler shift is given by

$$\Delta\nu = (2v/\lambda)\sin\tfrac{1}{2}\theta,$$

where $\Delta\nu$ = Doppler shift, v = velocity of particle in the direction along the bisector of the incident and scattered beams, θ = scattering angle and λ = wavelength of radiation in the scattering fluid.

The type of dopplermeter employed by the author differs somewhat from the earlier dopplermeters described. It is claimed that it is very easy to set up and gives a very good signal-to-noise ratio. The instrument has been described in detail elsewhere (Rudd 1969*b*, *c*) and therefore only a brief description will be given here. The dopplermeter is illustrated in figure 1. The parallel output from the laser is diverged by the microscope objective lens L, to cover the mask M. This mask contains two slits and in consequence produces two beams. These two beams are then focused by a single lens L_2 onto the fluid whose velocity is to be determined. Both beams are focused by the same lens, and so, provided it is free from aberrations, they must be brought to a focus and overlap at the same point. Thus the system may be said to be 'self-aligning'. This not only makes the system easy to set up but renders it very insensitive to vibration. Finally, the

beams which are transmitted by the fluid are collected by a third lens L_3 and detected by a solid state photodiode. A solid state device is used because the signal-to-noise ratio is sufficiently high for a photo-multiplier, with its attendant complications, to be unnecessary.

There is an alternative way of looking at the operation of the instrument which differs from the usual 'Doppler model'. This has already been published (Rudd 1969*a*) and is referred to as a 'Fringe model'. When the two light beams are brought to a mutual focus they interfere with each other. The interference pattern will be a set of fringes rather analogous to those produced by the Young's slits experiment. These fringes will lie parallel to the bisector of the two beams. As a scattering particle crosses these fringes it blocks off a varying amount of

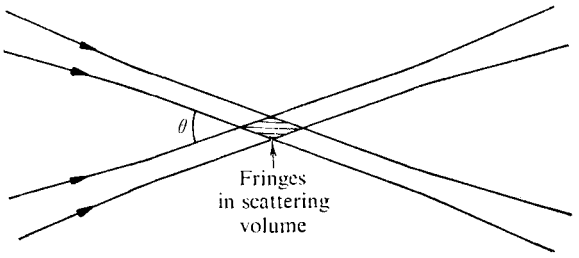

FIGURE 2. Fringes in the scattering volume.

light. If it lies in a bright fringe it blocks off much light, in a dark fringe, only very little. Thus, as the particle moves over the fringes the intensity of the total transmitted light will fluctuate. The frequency of fluctuation will be determined by the fringe spacing and the velocity of the particle. The fringe spacing d is given by $d = \frac{1}{2}\lambda \sin(\frac{1}{2}\theta)$ (see figure 2) and so

$$\Delta\nu = v/d = (2v/\lambda)\sin\tfrac{1}{2}\theta,$$

which is the same result as yielded by the 'Doppler model'. A strong signal is obtained since it is proportional to the amount of light which is blocked off, that is all the light which is scattered and absorbed rather than just that light which is scattered through a small range of angles. The size of the scattering volume is about $10\,\mu\text{m} \times 100\,\mu\text{m} \times 1\,\text{mm}$.

The dopplermeter system is completed by feeding the amplified photo-detector signal into a Tektronix 1L5 spectrum analyser. The output from this was passed, via an integrating amplifier, onto a U, V chart recorder. The Doppler spectrum was measured up at a later time. The mean velocity was determined from the centre of the peak and the fluctuating velocity from the width of the peak. However the dopplermeter itself produces a widening of the peak, even for a steady velocity. This is because the fringe pattern in the scattering volume has a finite extent and hence the Doppler pulse from each scattering particle has a finite length. This inherently gives rise to a broadening of the Doppler spectrum of typically 6–7 %. Corrections for this line width are made in measuring the turbulent intensities. This is done by taking the square root of the difference of the squares of the measured and the inherent line widths. This may be justified by Fourier transform theory with the use of Parseval's theorem.

3. Experimental measurements for polymer solution

To date, the most common method of measuring velocities in dilute polymer solutions has been to use Pitot-static tubes or hot-wire or hot-film probes. Serious objections can be raised concerning these instruments (Friehe & Schwarz 1969) because of the visco-elastic forces present in the fluid. These can either introduce extra normal stresses, which the Pitot-static tube measures, or else modify the flow regime around the hot wire or film so that the heat conduction is modified. Thus the reliability of the measurements by Virk *et al.* (1967) and Spangler (1969) can be questioned. Seyer & Metzner (1969) have attempted to overcome this difficulty by measuring the velocities of small air bubbles suspended in the fluid. However, this method is extremely tedious.

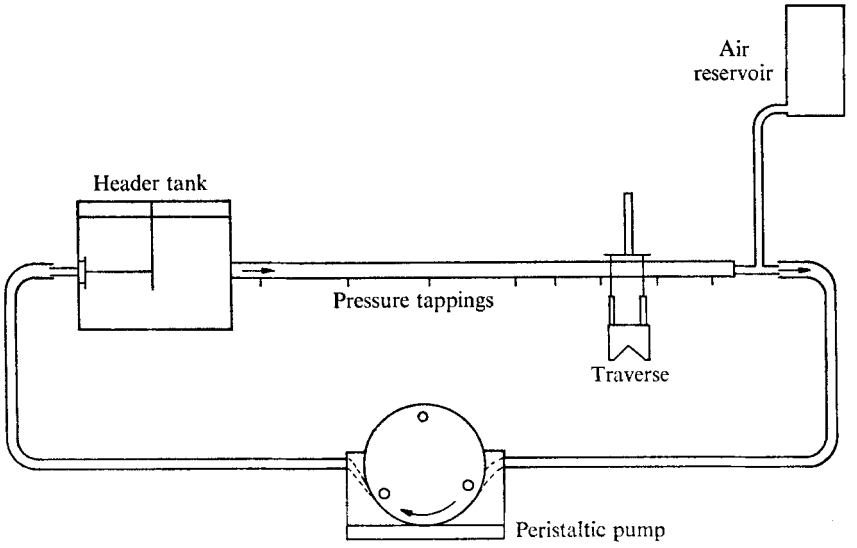

FIGURE 3. Flow system for experiments, not to scale.

The laser dopplermeter appears most promising since it does not interfere with the flow. Also, it has been found that, at a concentration of 100 p.p.m. or so, the polymer molecules produce quite a significant amount of light scattering and thus one is measuring the velocity of the molecules themselves. For example, if the molecules produce a refractive index change of 1 part in 10^5, then a phase shift of the laser beam of about 0·01 radians is produced and this can easily be detected. Further, the effect of the polymer solution was thought to manifest itself upon the viscous sublayer and thus the extremely good spatial resolution of which the instrument is capable should prove of great value in studying this layer. Finally, the dopplermeter is inherently a linear instrument and thus capable of measuring the very high turbulent intensities that are present in the viscous sublayer without the need to apply large corrections.

One slight disadvantage of the instrument is that it is necessary to view the flow through a plane window in order to avoid spherical aberration. This means that the pipe employed must be square. As a consequence there will be some

secondary flow, but this is not thought to be significant for reasons given at the end of this section.

The main experiment conducted with the dopplermeter was the comparison of a Newtonian and a drag-reducing fluid in pipe flow. For this purpose a special rig was built (figure 3). The pipe itself was a $\frac{1}{2}$ in. square, 7 ft 6 in. long Perspex pipe with pressure tappings placed at intervals along its length. The pipe was counterbalanced at one end to try to stop it sagging and hence prevent it from inducing secondary flow. The polymer employed for drag reduction is very susceptible to degradation (fracture of the molecules), and a normal centrifugal

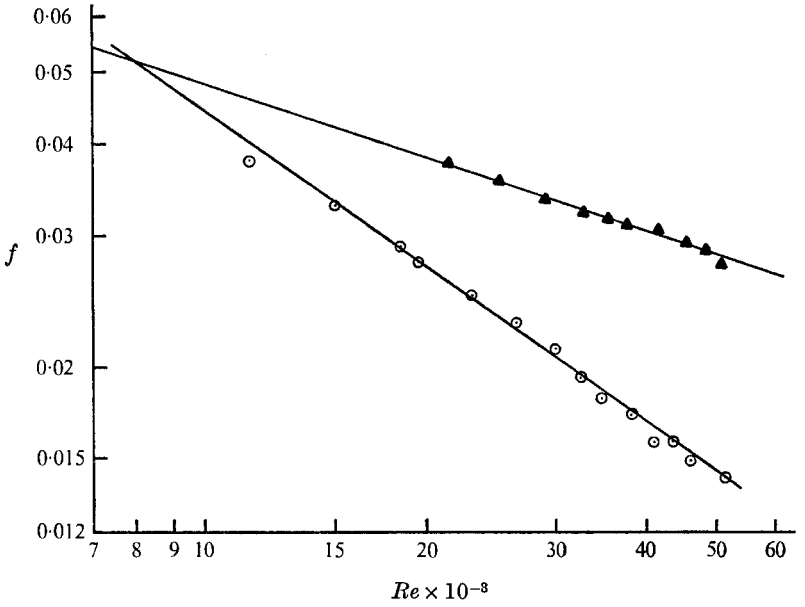

FIGURE 4. Friction factor versus Reynolds number. ▲, water; ⊙, 0·01 % Separan; $(U_\tau)_{\text{crit}} = 0{\cdot}032$ m/sec.

pump was found to be too severe for it. Therefore a special peristaltic pump was used. This operates by squeezing the polymer along a flexible pipe by means of a roller and a semicircular track. This pump also produces very severe pressure and velocity fluctuations as the rollers go onto and come off the track and provision had to be made to absorb these. This was done by providing a $\frac{1}{2}$ ft^3 header tank above the pipe and a 1 ft^3 sealed air reservoir at the end of the pipe. These reduced the pulsations to a level which was not considered significant. The tops of the manometers, connected to the pressure tappings, were connected via a tap to the air reservoir to enable the pressure above the manometers to be reduced. This is necessary since the pressure in the pipe is well below atmospheric.

The peristaltic pump was driven by a fixed speed motor, but control of the flow rate could be achieved both by varying the gap between the rollers and track and also by partially clamping the pipe. Large changes in the flow rate could also be achieved by changing the diameter of the flexible pipe in the pump, both 1 in. and $1\frac{3}{4}$ in. diameter pipes were employed.

The first measurement to be taken was a pressure profile down the length of the pipe. The pressure gradient was found to be sensibly uniform over the working section as might be expected since it is 120 widths from the entrance.

Next the friction coefficient was measured as a function of Reynolds number (figure 4) for both a Newtonian fluid (tap water) and a drag-reducing fluid (100 p.p.m. Separan AP 30). Separan AP 30 is a polyacrylamide and was chosen since it is quite an effective drag-reducing agent and not too susceptible to degradation. Polyox is more effective for drag reduction but is much more easily broken up. Indeed the peristaltic pump was not found to have any effect on the polyacrylamide, but destroyed the Polyox in 5 or 10 min. The only degradation of the polyacrylamide was a long-term one, about 10% overnight, and was probably due to biological action. In figure 4 the dramatic drag-reducing effect is clearly demonstrated.

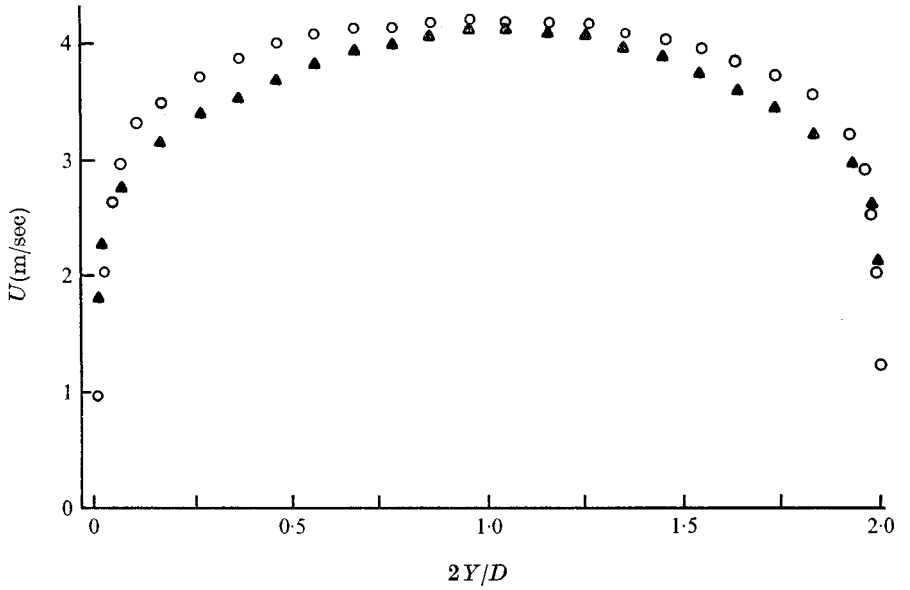

FIGURE 5. Velocity profile across pipe. ▲, water; ○, 0·01% Separan.

Measurements were next conducted with the dopplermeter and results for mean velocity profile and axial turbulent intensity were obtained. These are shown in figures 5 and 6. Measurements were made to within 0·006 in. of the wall. This was not quite as close as with an earlier pipe, possibly because the walls were contaminated by the chloroform used to cement the Perspex together.

Finally an experiment was conducted to try to measure the spanwise velocity fluctuations in the pipe flow (figure 7). This was done by rotating the whole optical bench through an angle θ about a vertical axis so that the velocimeter was sensitive to both axial and spanwise velocities. Astigmatism was produced since the light beam did not enter the pipe normally. This would usually cause complete loss of Doppler signal if the beam were canted by more than 15°–20°, because the fringe pattern becomes too distorted. However, this can be compensated for by

inserting a Perspex block whose incremental optical path length is approximately equal to half that produced by the pipe, and placing it on the laser side of the pipe. It is then rotated about a horizontal axis by the same angle as the bench was rotated about a vertical axis. This proved to be very effective and there was no sensible signal loss up to quite large angles of rotation.

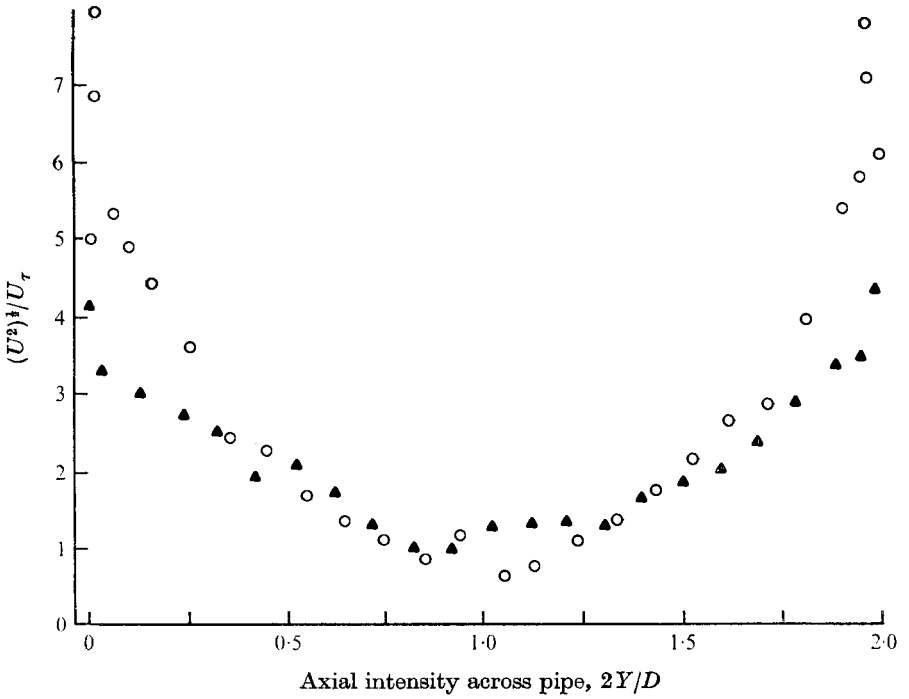

FIGURE 6. Intensity of the axial turbulent velocities across the pipe. ▲, water; ○, 0·01 % Separan; U_τ = 0·1 m/sec.

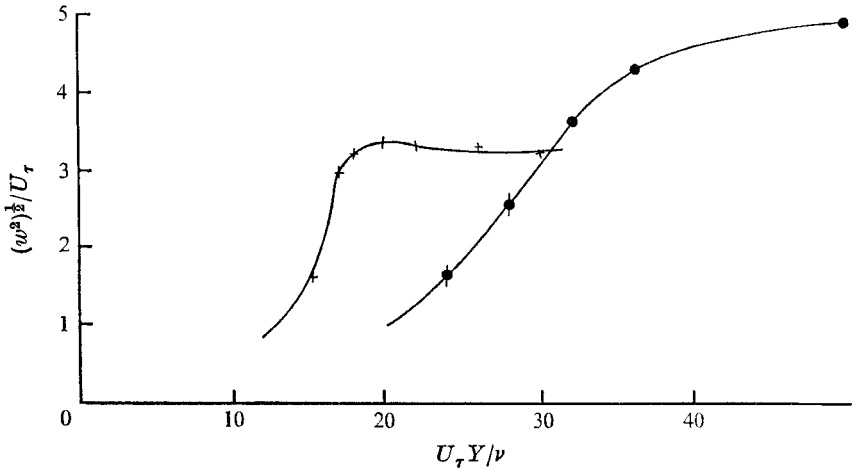

FIGURE 7. Intensity of the tangential turbulent velocities across the pipe. +, water; ●, 0·01 % Separan.

4. Discussion of experimental results

The experimental results obtained in the previous section will now be considered in terms of the usual turbulence theory (Townsend 1956). Lumley (1969) has shown that the results do not differ from those for Newtonian fluids as much as might at first be thought. The turbulence in a pipe consists of a central core region, where the inertial forces are dominant, and a thin wall region, called the viscous sublayer, where the viscous stress dominates. The effect of the polymer additive will be shown to be restricted to a narrow region on the edge of the viscous sublayer.

In fully turbulent flow with a high Reynolds number the structure of the flow is determined by the large eddies with a scale comparable to that of the flow. These eddies break down by a cascade process into smaller eddies and eventually the energy is dissipated by very small eddies due to viscosity. The scale of these eddies for a Newtonian fluid was given by Kolmogoroff as $(\nu^3/\epsilon)^{\frac{1}{4}}$, where ϵ is the rate of dissipation of energy per unit mass and ν is the kinematic viscosity. The large eddies are not coupled to these small dissipating eddies and therefore their structure is independent of the nature of the dissipation. That is to say, the eddies which contain the energy and determine the Reynolds stresses are not directly affected by viscous forces, either Newtonian or non-Newtonian. Their rate of energy loss and motion does not depend upon the rheological properties of the fluid but only upon the boundary conditions at the edge of the region of the fully turbulent flow.

If the viscous layers near the walls of the pipe are thin, the fully turbulent region occupies almost the whole of the channel and the boundary conditions are provided by the pressure gradient along the pipe and the constraint of the walls. For channels of similar sectional shape we have a generalized expression for the mean velocities U, v and w, the axial, radial and tangential components respectively.

$$U = U_1 - U_\tau F(Y/D, Z/D),$$

$$v = U_\tau - g(Y/D, Z/D),$$

$$w = U_\tau - h(Y/D, Z/D),$$

where $U_\tau = (\tau_0/\rho)^{\frac{1}{2}}$, U_1 = axial velocity at the centre, X = distance along the axis of the pipe, Y = distance from wall, Z = third dimension, τ_0 = wall stress and ρ = density of fluid. The first equation is known as the 'velocity defect law'. This is valid for any kind of molecular dissipation process. The only limitation is that the Reynolds number must be large enough for a cascade process to exist and for the energy dissipation to take place on a scale which is small compared with the mean scale of the turbulent motion.

The results obtained for water and the polymer solution are plotted in figure 8, where $(U_1 - U)/U_\tau$ is plotted against Y/D. The two are seen to not differ significantly. A similar conclusion was reached by Virk *et al.* (1967). The reason for the flatter drag reducing profile in figure 5 is that, since the wall stress is lower, the velocity defect is less at a similar position in the flow. The polymer additive does not have any affect upon the turbulence in the core region of pipe flow. The change in the profile is solely due to the change in the wall stress. This suggests that the effect of the additive is confined to the region of pipe flow close to the wall.

The velocity profile close to the wall may be represented by the law of the wall (Townsend 1956). For a non-Newtonian fluid this must be modified (Seyer & Metzner 1969), as has also been discussed by Lumley (1969). For a fluid with a 'viscosity' described by ν and time parameters θ, Φ etc. it becomes

$$U = U_\tau F(U_\tau Y/\nu, U_\tau^2\theta/\nu, \Phi/\theta, \ldots).$$

For large values of $U_\tau Y/\nu$ we know that (Townsend 1956), $dU/dY = AU_\tau/Y$, where A^{-1} = von Kármán's constant and so

$$U = AU_\tau\{\log(U_\tau Y/\nu) + B(U_\tau^2\theta/\nu, \Phi/\theta)\},$$

where B is a function particular to the material.

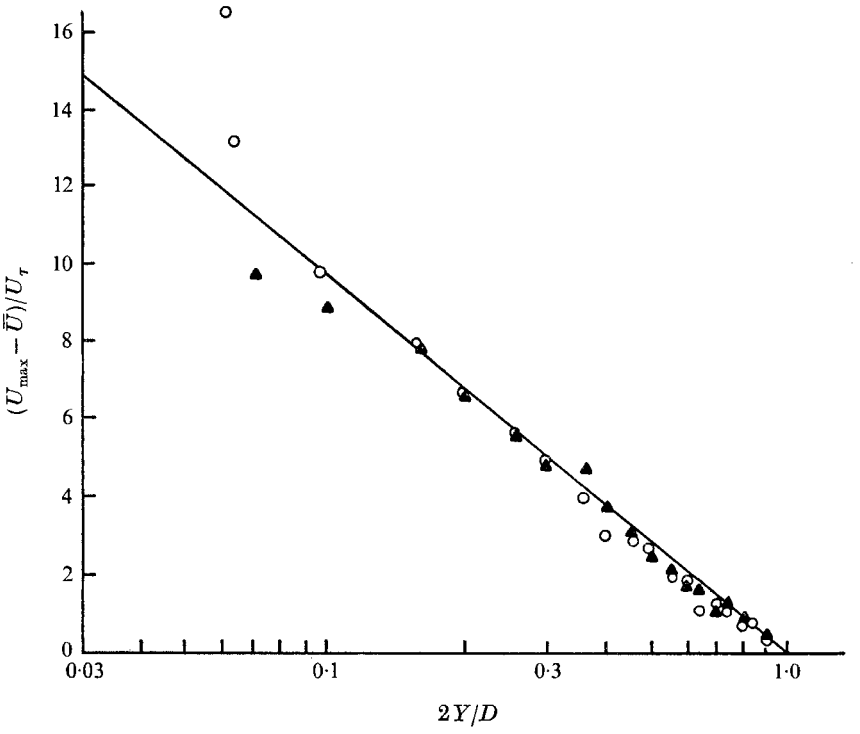

FIGURE 8. Velocity defect law for the pipe. ▲, water; ○, 0·01 % Separan.

Combining this with the defect law, the maximum velocity U_1 at the centre of the pipe, $Y = \frac{1}{2}D$, is given by

$$U_1 = AU_\tau(\log U_\tau D/\nu) + B - C),$$

where C depends only upon the full turbulent flow and is independent of the fluid. Clearly, an increase in the value of B will appear as an increase in the flow for the same wall stress, which is equivalent to drag reduction.

A simple representation of the wall layer is to combine a viscous sublayer, with the velocity profile

$$U = U_\tau^2 Y/\nu,$$

with the logarithmic profile, without any transition layer between them. If the

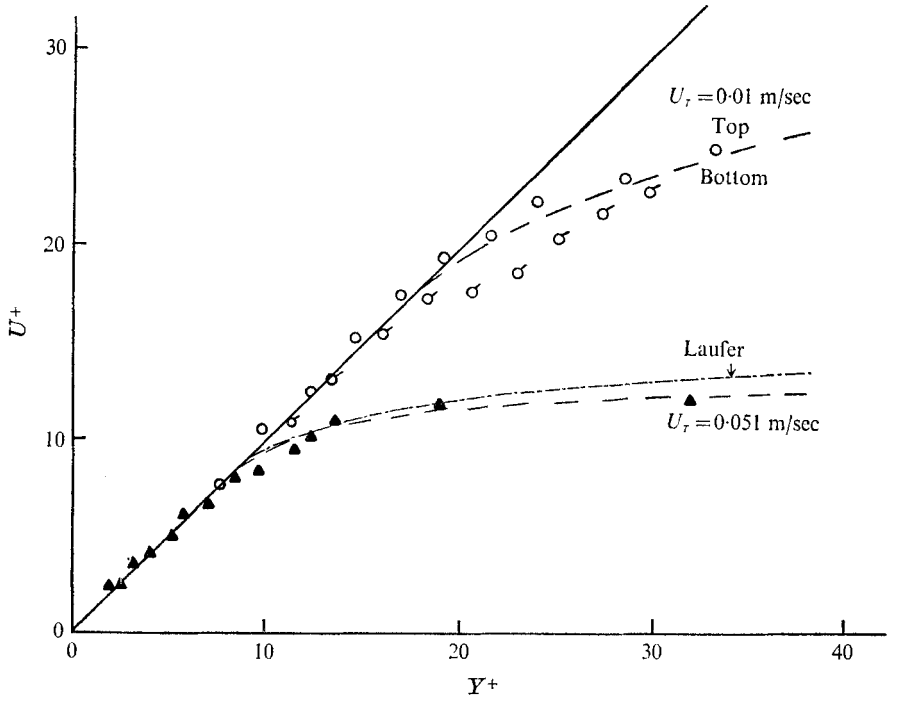

FIGURE 9. Velocity profile in viscous sublayer, close to pipe wall. ▲, water; ○, 0·01 % Separan (top wall); ♂, 0·01 % Separan (bottom wall).

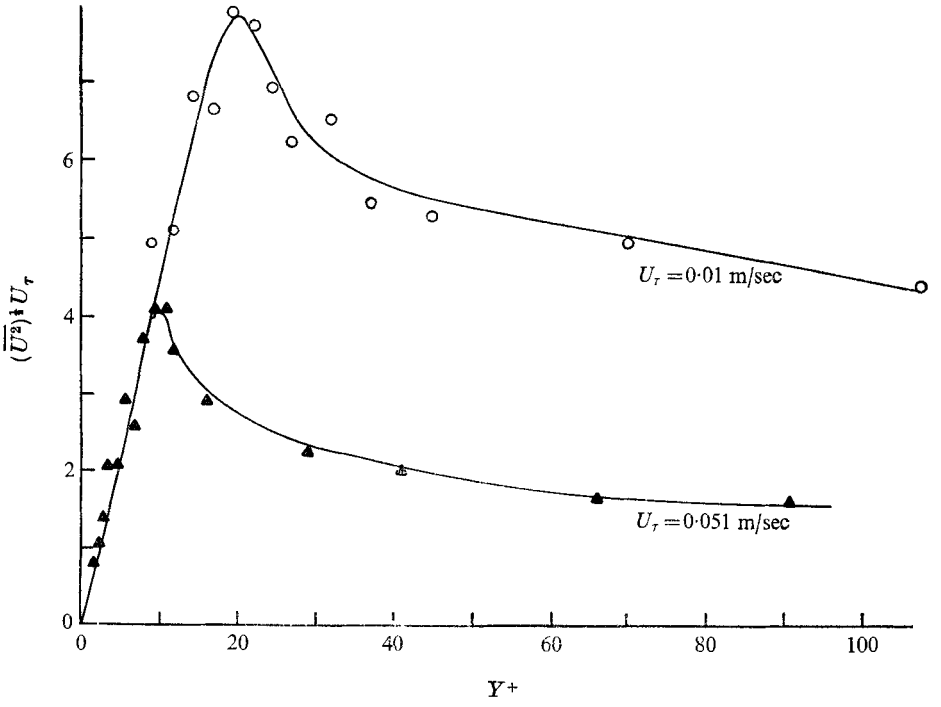

FIGURE 10. Intensity of axial turbulent velocities in viscous sublayer, close to pipe wall. ▲, water; ○, 0·01 % Separan.

junction occurs at the non-dimensional position $U_\tau Y/\nu = \alpha$ then $B = \alpha - A \log \alpha$. α is then a critical 'Reynolds number' for the stability of the viscous layer and any increase in stability of this layer will increase α and so increase B. $U^+ (= U/U_\tau)$ is plotted against $Y^+ (= U_\tau Y/\nu)$ for the wall region of both water and a polymer solution in figure 9. A considerable difference between the two is seen. The region where $U^+ = Y^+$ (the viscous sublayer) is considerably extended in the case of the polymer solution. The effect of the additive is to thicken the viscous sublayer so that a greater velocity arises in the centre of the pipe for the same wall stress. Conversely, a lower wall stress is required for the same maximum velocity in the pipe and so drag reduction occurs.

The non-dimensional axial component of the fluctuating velocity is plotted against Y^+ in the wall region in figure 10. A plot over the whole pipe has already been shown in figure 6. There is not thought to be any significant difference for the two fluids in the centre of the pipe, where Reynolds stresses dominate. However, in the wall region the drag-reducing solution has a considerably *greater* turbulent intensity than the Newtonian fluid. Figure 10 shows that the increase in intensity is directly proportional to the thickening of the sublayer. The intensity inside the sublayer is, however, constant for both fluids, when expressed in terms of the local mean velocity, and is around 35–40 %. This has recently been confirmed by diffusion measurements of Fortuna & Hanratty (private communication). This suggests that only the scale of the sublayer and not the basic structure of the turbulence, has changed. Note that U^+ depends only upon the distance from the wall and not upon the fluid or the Reynolds number.

The plot of the spanwise component of the fluctuating velocity against Y^+ in the wall region has been shown in figure 7. At some distance from the wall the intensity in the drag-reducing solution is again higher than that of the Newtonian fluid. However, close to the wall and inside the viscous sublayer the drag-reducing solution has a lower intensity. This suggests that the sublayer is thickened by the spanwise component being suppressed, which in turn stabilizes the eddies close to the wall.

5. Summary of results

Rudd (1971) has shown that the non-Newtonian velocity profiles can be rescaled by employing a pseudo-viscosity of D_0 times the kinematic viscosity. The factor D_0 is defined by

$$D_0 = (1 + KDe)^{\frac{1}{2}},$$

where

$$De = \text{Deborah number} = \theta u_\tau^2 \rho/\nu,$$

$$\theta = \text{relaxation time of molecules}, \quad K \approx 0{\cdot}5.$$

Thus U_τ becomes $D_0 u_\tau$, U^+ becomes U^+/D_0 and Y^+ becomes Y^+/D_0. A plot of the rescaled velocity profiles for the viscous sublayer, where the fluid stress is sensibly constant, is given in figure 11. The data are seen to collapse very nicely.

The polymer additive does not have any significant effect on the central region of pipe flow, which confirms Reynolds number similarity predictions. The drag-reduction mechanism is confined to the viscous sublayer close to the wall where the rate of shear is a maximum. The layer is thickened to give a greater

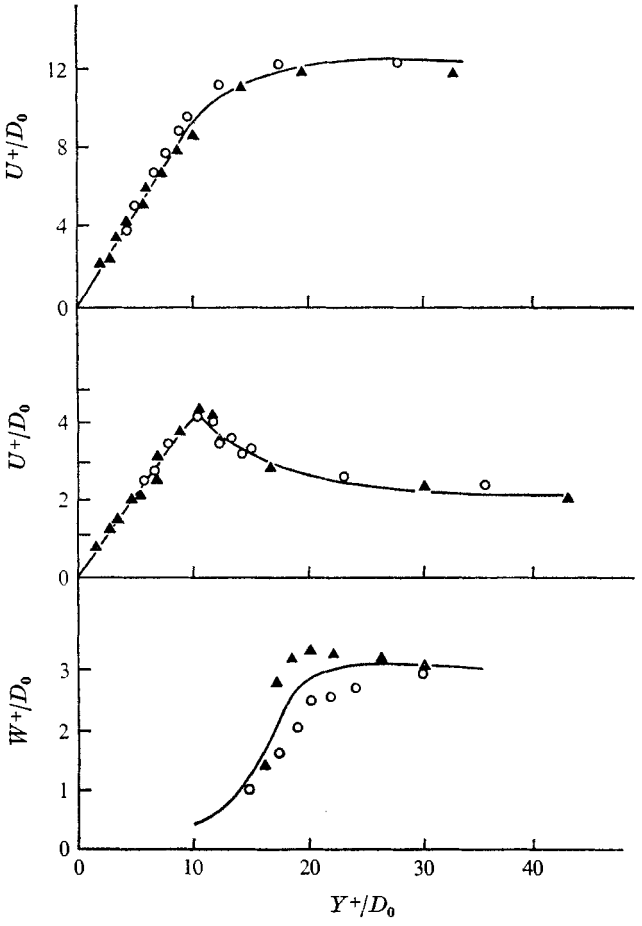

FIGURE 11. Rescaled velocity profiles in viscous sublayer close to pipe wall. ▲, water; ○, 0·01 % Separan; $D_0 = (1+KDe)^{\frac{1}{2}}$.

flow rate for the same wall stress, or lower wall stress for the same flow rate. The additive does *not* induce a general suppression of turbulence in the sublayer and indeed in one sense the axial component is unchanged. However, very close to the wall the spanwise component is *suppressed* and this in turn stabilizes the turbulence, causing larger Townsend 'roller' eddies to exist at the wall than for a Newtonian fluid.

The author wishes to thank Dr A. A. Townsend and Dr B. M. Watrasciewicz for their constant help and encouragement and Professor A. B. Metzner for interesting the author in this subject.

REFERENCES

BRUNDETT, E. & BAINES, W. D. 1964 *J. Fluid Mech.* **19**, 375–394.

FRIEHE, C. A. & SCHWARZ, W. H. 1969 *Viscous Drag Reduction* (ed. C. Sinclair Wells), pp. 281–296. Plenum Press.

FOREMAN, J. W., GEORGE, E. W., FELTON, J. L., LEWIS, R. D., THORNTON, J. R. & WATSON, H. J. 1966 *J. Inst. Elec. Electron Eng. Q.E.* **2**, 260.

GOLDSTEIN, R. J. & KREID, D. K. 1967 *J. Appl. Mech.* **34**, 813.

LUMLEY, J. L. 1969 *Annual Review of Fluid Mechanics*, vol. 1, p. 367. Annual Reviews Inc.

METZNER, A. B. & PARK, M. G. 1964 *J. Fluid Mech.* **20**, 291–325.

RUDD, M. J. 1969*a* *J. Sci. Instrum.* **2**, 55.

RUDD, M. J. 1969*b* *Optics Technology*, **1** 264.

RUDD, M. J. 1969*c* *Nature*, **224**, 587.

RUDD, M. J. 1971 Drag reduction. *Ch.E. Progress Symp. Series*, no. 11, vol. 67.

SEYER, F. A. & METZNER, A. B. 1969 *A.I.Ch.E.* **15**, 426–35.

SPANGLER, J. G. 1969 *Viscous Drag Reduction* (ed. C. Sinclair Wells), pp. 131–358. Plenum Press.

TOMS, B. A. 1949 *Proc.* (*First*) *Int. Congr. on Rheology*, vol. 2, p. 135. Amsterdam: North Holland Pub-Co.

TOWNSEND, A. A. 1956 *The Structure of Turbulent Shear Flow*. Cambridge University Press.

VIRK, P. S., MERRILL, E. W., MICKLEY, H. S., SMITH, K. A. & MOLLO-CHRISTENSEN, E. L. 1967 *J. Fluid Mech.* **30**, 305–328.